TRANSACTIONS OF THE INSTITUTE OF FLUID-FLOW MACHINERY

No. 125, 2013, 13–28

KAROL RONEWICZ*, TOMASZ TURZYŃSKI, DARIUSZ KARDAŚ

Design and distribution of air nozzles in the biomass boiler assembly

The Szewalski Institute of the Fluid-Flow Machinery Polish Academy of Sciences, Fiszera 14, 80-231 Gdańsk, Poland

Abstract

Due to energy crisis as well as increasing pollution of the enviroment, renewable energy sources usage increases all over the world. These facts encouraged authors to start research over developing a uniform biomass boiler calculation model. Paper presents the design of biomass boiler assembly created for the organic Rankine cycle unit since these systems could achieve strong position in energy industry. To achieve optimal performance of boiler assembly, two additional devices have been designed: the economizer and air preheater. Such installation allows to reach the assembly efficiency of 82%. The research over the air nozzles placement in the combustion chamber in order to ensure the best firebox efficiency is also presented. Modeling is based on computational fluid dynamics simulations of pyrolysis on the moving grate. Released gases are being transported to the combustion chamber, mixed with air from the nozzles and combusted. Furthermore, the model assumes different distribution and composition of gases across the moving grate.

Keywords: Biomass; Boiler assembly; CFD, Combustion; Design; Firebox

Nomenclature

A	–	heat transfer area
H	–	height of the firebox
k	–	heat transfer coefficient
K_1	–	canal inside the inner helical coil of the exchanger
K_2	–	canal between the inner and outer helical coils of the exchanger
P♯1–P♯5	–	number of the air preheater canal
P_1	–	inner helical coil of the exchanger
P_2	–	outer helical coil of the exchanger
Q_a	–	air heat rate

*Corresponding author. E-mail address: kronewicz@imp.gda.pl

Q_c	–	coolant heat rate
Q_e	–	heat exchange rate between flue gases and coolants
Q_{fg}	–	heat rate removed from flue gases
Q_o	–	oil heat rate
T_{a0}	–	initial temperature of air
T_{af}	–	final temperature of air
T_{fg0}	–	initial temperature of flue gases
T_{fgf}	–	final temperature of flue gases
T_{o0}	–	initial temperature of oil
T_{of}	–	final temperature of oil
ΔT_1	–	difference between initial temperature of flue gases and final temperature of oil
ΔT_2	–	difference between final temperature of flue gases and initial temperature of oil
ΔT_m	–	logarithmic difference of temperature between ΔT_1 and ΔT_2,
w_{fg0}, w_{fg}, w_{fgf}	–	velocity value of flue gases: initial, mean, and final
w_{o0}, w_o, w_{of}	–	velocity value of oil: initial, mean, and final
w_{a0}, w_a, w_{af}	–	velocity value of air: initial, mean, and final
W1,W2	–	respectively second and first draft of the economizer
V_x	–	vertical component of mean velocity

1 Introduction

This paper presents a design of biomass boiler assembly created for 100 kW organic Rankine cycle (ORC) unit. Due to low turbine set efficiency, in order to achieve 100 kW of electrical power, it is required that the boiler assembly provides 600 kW of power in heat. This work focuses solely on the biomass boiler assembly.

Boiler has been designed to be able to use vast variety of fuels characterized by low calorific value and high amount of moisture (up to 30%). This requires that a 3-sectional moving grate is installed in the firebox to ensure the total combustion of biomass fuel. The heating agent needs to achieve optimal parameters for the heat exchange with the ORC low-boiling agent. These are: $T_{o0} = 245\,^{\circ}\mathrm{C}$, $T_{of} = 295\,^{\circ}\mathrm{C}$. In order to meet such parameters, thermal oil has been chosen as the heating agent in this assembly. All the calculations have been made for the case of the Shell Thermia B thermal oil physical properties.

2 Firebox

The firebox design was created based upon analytical calculations considering low calorific fuels containing large amount of moisture (up to 30%). To deal with such fuel, the combustion chamber was equipped with 1.6 m long moving grate system to ensure optimal drying, gasification and afterburning charcoal. The moving grate is comprised of six rows of fixed grate bars and six rows of moving bars, ten and eleven bars each. Grate air is being distributed in three

sections independently allowing full control over combustion process on the grate. Moreover, the combustion chamber was equipped with two separated secondary air nozzles, creating a swirl and thus prolonging the particle residence time. The inside of the chambers steel body was isolated with the fireproof chamotte bricks, while the outside surface should be isolated with high temperature glass wool and coating. The firebox schematic was presented in Fig. 1.

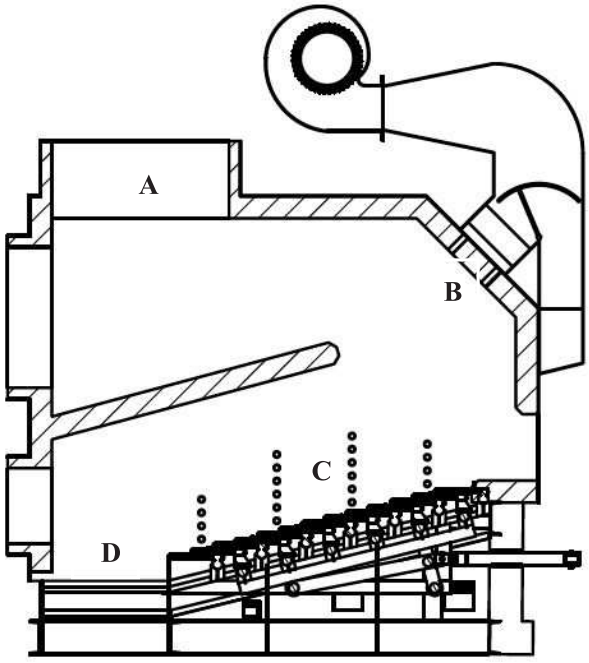

Figure 1. Moving grate biomass combustion chamber. A – flue gas outflow, B – secondary air additional nozzles, C – secondary air nozzles, D – ash chute.

3 Exchanger

Heat exchanger unit was designed as two steel coaxial helical coils, 42 coils each. The main exchanger schematic was presented in Fig. 2. Flue gas inlet is located at the top of the construction. Hot gases travel downward, exchanging heat with oil in the smaller coil, then change direction and travel up between both coils and finally to the stack. Oil inlet is located at the top of the exchanger in the outer coil and oil outlet is located at the top of the inner coil. This geometry defines the mixed-type exchanger in which there are both counter-current and counter/co-current mixed zones.

Knowing that the flue gas flow will most likely contain a large amount of

particles (ash, unburned fuel parts or other impurities), the exchanger chamber was equipped with a chute connected with safety valve with pressure compensation. This particular heat exchanger was designed to acquire about 450 kW of heat from the hot gases, which enables achieving thermal oil parameters on outlet and inlet of 258 °C and 295 °C respectively. While the outlet parameter seems fine, the inlet temperature of the heating agent is too high. To obtain designed parameters it was necessary to make a design of the economizer, which will raise plant's efficiency and supply required oil parameters at the inlet.

4 Economizer

The economizer was designed to be a device that absorbs heat from the low enthalpy flue gases and uses it to raise the oil temperature from the desired 245 °C to the inlet temperature for the main exchanger (258 °C). Thermal oil flows through a set of four double coaxial coils, similar to the coils used in the main heat exchanger. Furthermore, the construction is divided into two strictly cocurrent zones. Flue gas inlet is located at the top of the smaller coil set section. The hot stream of gases moves downward perfusing coil pipes and exchanging heat. Then, at the bottom, flue gases flow into larger coil set section and flow upward to the stack. Oil flow direction is always opposite to the flue gas flow, making the economizer a typical countercurrent exchanger. In this case, similarly to the main heat exchanger, the primary chamber of the economizer was equipped with a chute connected with the safety valve with pressure compensation. The scheme of economizer was presented in Fig. 3.

While the oil parameters were achieved, the problem of flue gas high outlet temperature appeared. The preheater seemed to be necessary to make use of this waste heat air.

5 Air preheater

Air preheater is a device that closely resembles a cross flow shell and tube exchanger. Flue gas flow is divided between 400 separate pipes with internal diameter of 59.3 mm and total length 2.1 m. Five air channels inside of which the cold air perfuses the pipes and thus heats itself up before entering the firebox are perpendicular to the pipes. The flow directions and geometry of the air cooler is presented in Fig. 4.

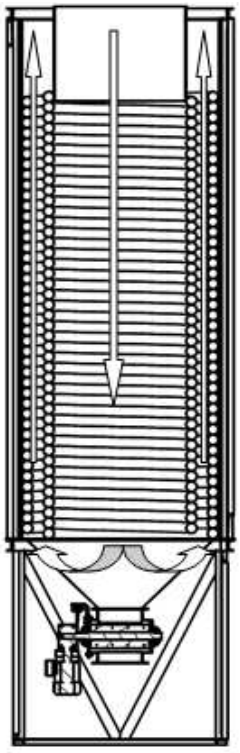

Figure 2. Main heat exchanger and flue gas flow diagram.

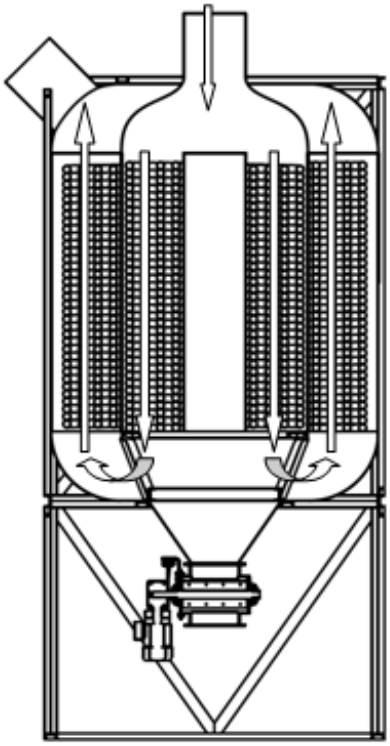

Figure 3. The economizer and flue gas flow diagram.

6 Energy balance of the assembly

Based on the literature [1,2,3] and authors previous work [4,5], energy balance calculations for boiler assembly were conducted. Using required oil parameters, shape and heat transfer area of the assembly were calculated [4]. The results of these calculations are presented in this work.

As it is shown in Tab. 1, thermal oil has reached the required temperature of $T_{of} = 295$ °C after receiving $Q_o = 602.7$ kW of energy. The air while preheating up to $T_{af} = 138.6$ °C has received $Q_a = 67.3$ kW of energy. The flue gases have exchanged a total of $Q_{fg} = 669.3$ kW of energy, while the cooling agents (thermal oil and air) received $Q_c = 670$ kW of energy.

Figure 5 shows the cross-section of the biomass helical coil boiler. Flue gases flow out of the firebox to the boiler's upper inlet, from there towards the bottom and then again back to the top outflow. After the heat exchange, gases are directed to the economizer, followed by air preheater. Thermal oil, on the other hand, is at first preheated in the economizer and after that is directed to the

boiler's outside helical coil's upper part. The cooling agent exchanges heat with flue gases while flowing towards the bottom of the outer coil, then enters the inner coil and flows towards the upper outflow.

The heat is exchanged in cocurrent as well as in countercurrent processes. As the flow diagram in Fig. 5 shows, on the inner area of the inner coil (P1-K1) as well as on the inner area of the outer coil (P2-K2) the heat exchange process is countercurrent. On the outer area of inner coil (P1-K2) the heat exchange process is cocurrent.

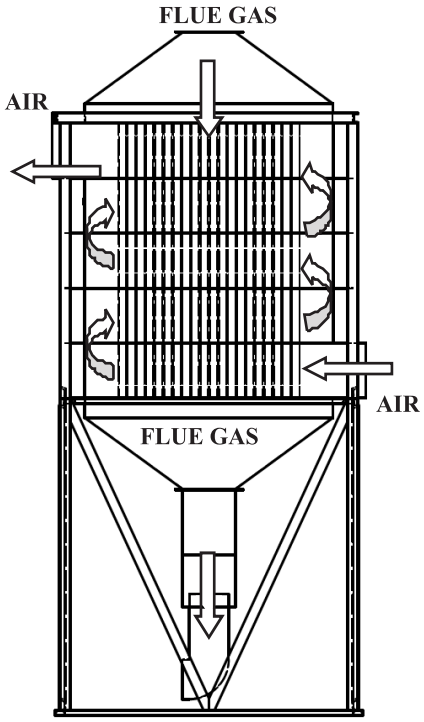

Figure 4. Air preheater with flue gas and air flow diagram.

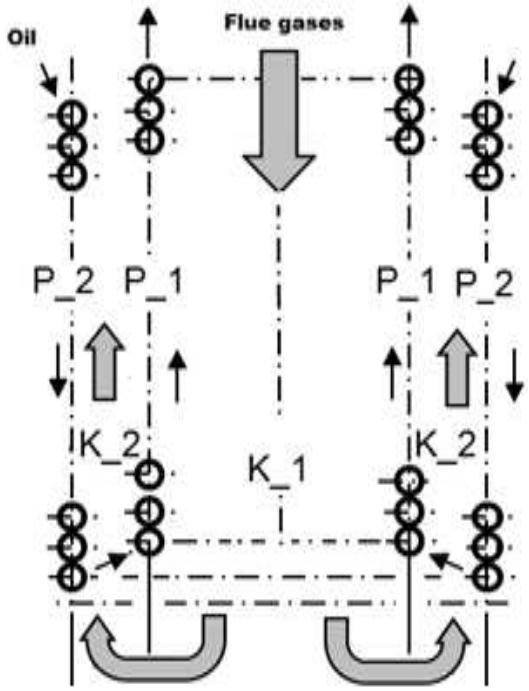

Figure 5. The cross-section biomass boiler as well as flue gases flow (grey arrows) and thermal oil flow (black arrows) diagram. Designations according to nomenclature.

Figure 6 shows the cross-section of the economizer. In this device, thermal oil flows inside the series of helical tubes while flue gases flow between them inside two canals. Flue gases flow is marked with grey arrows, while the cooling agent flow is marked with black arrows. Figure 7 presents the cross-section of air preheater. In this case air is the cooling agent and washes the bundle of straight tubes with flue gases flowing inside.

Table 1. Mass and energy balance calculations results [4,5]. The designations according to nomenclature. $\Delta T_1 1 = T_{fg0} - T_{of}$, $\Delta T_2 = T_{fgf} - T_{o0}$, ΔT_m – logarithmic mean temperature difference between ΔT_1 and ΔT_2.

Flue gases' heat						
Canal	T_{fg0}	T_{fgf}	w_{fg0}	w_{fg}	w_{fgf}	Q_{fg}
Unit	°C	°C	m/s	m/s	m/s	kW
K_1	1083.15	747.7	3.58	3.1	2.68	252.23
K_2	747.70	478.0	6.72	5.84	4.93	192.33
W_2	478.00	271.0	0.87	0.83	0.63	143.8
W_1	271.00	251.5	0.95	1.82	0.92	13.67
Preheater	251.50	151.5	1.0	0.93	0.86	67.30
Sum	–	–	–	–	–	669.30
Heat received by thermal oil						
Canal	T_{o0}	T_{of}	w_{o0}	w_o	w_{of}	Q_o
Unit	°C	°C	m/s	m/s	m/s	kW
P_1	266.40	295.00	1.67	1.67	1.67	348.07
P_2	258.24	266.40	1.64	1.64	1.64	97.16
W_1	245.00	246.14	0.87	0.83	0.63	143.80
W_2	246.14	258.24	0.95	1.82	0.92	13.67
T. Oil heat	–	–	–	–	–	602.70
Heat received by air						
	T_{a0}	T_{af}	w_{a0}	w_a	w_{af}	Q_a
Unit	°C	°C	m/s	m/s	m/s	kW
Preheater	20.00	138.60	0.95	1.10	1.25	67.3
Sum (oil and air)	–	–	–	–	–	670.00
Heat exchange on all heating surfaces						
Canal	ΔT_1	ΔT_2	ΔT_m	k	A	Q_e
Unit	K	K	K	W/m^{2}K	m^2	kW
P_1-inner	788.0	481.0	622.00	28.50	15.77	280.00
P_1-outer	481.0	183.0	308.00	14.45	15.77	70.00
P_2-inner	481.0	211.0	326.00	14.40	20.50	97.00
W_1	25.5	6.5	13.90	18.10	53.39	13.67
W_2	219.8	25.5	90.0	14.90	107.32	143.70
$P\sharp 1$	136.5	92.9	133.30	3.60	31.83	13.80
$P\sharp 2$	140.1	96.5	116.95	3.46	31.83	13.40
$P\sharp 3$	143.8	100.1	120.70	3.29	31.83	13.10
$P\sharp 4$	147.6	103.8	124.40	3.10	31.83	12.90
$P\sharp 5$	151.5	107.6	128.30	2.98	31.83	12.67
Sum	–	–	–	–	–	670.00

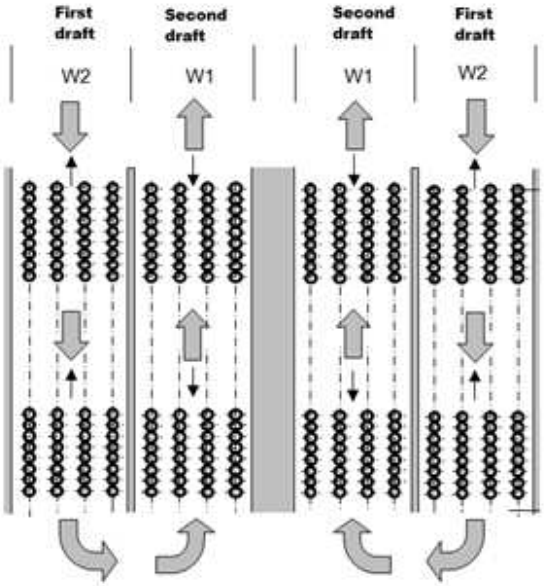

Figure 6. The cross-section of economizer as well as flue gases flow (grey arrows) and thermal oil flow (black arrows) diagram. Designations according to nomenclature.

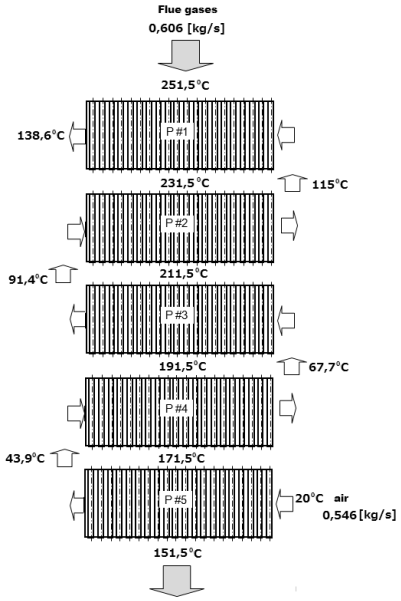

Figure 7. The cross-section of air preheater as well as air flow (white arrows) and flue gases flow (grey arrows) diagram.

7 CFD modeling of combustion and air nozzles placement in firebox

In addition to the design of boiler assembly and energy balance calculations, CFD modeling of the air nozzles placement has been simulated as well.
CFD calculations were conducted using the ANSYS software [6]. The computational domain closely resembles the combustion chamber (1:1 in scale) and consists of approximately 1 million cells. The following models were applied: p-1 model of radiation, k-ε model of turbulence (constant wall function), 1-equation model of combustion (finite rate/eddy dissipation). The gas density was calculated from the incompressible ideal gas model. Figure 8 shows the dimensions of the firebox presented previously in Fig. 1. The air delivered to the firebox has been divided in 40:60 ratio, where 40% of the air is delivered from under the grate and 60% through secondary nozzles (side and upper). During CFD modeling, three combinations of secondary air nozzle placements have been simulated:

- Case 1 – secondary air is introduced via side nozzles (Fig. 1 – C) only.
- Case 2 – secondary air is delivered via side and upper nozzles simultaneously

(divided so that equal amount of air flows through side nozzles and upper nozzles).

- Case 3 – secondary air is injected via upper nozzles (Fig. 1 – B) only.

The primary air was delivered to the firebox in the same amount in every case.

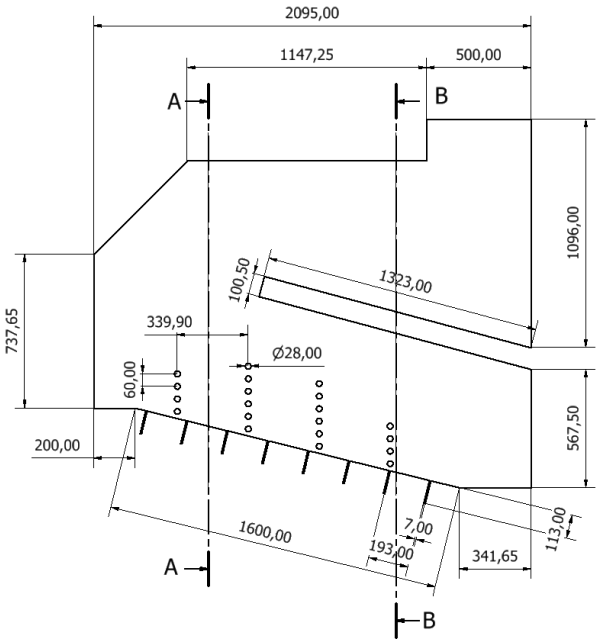

Figure 8. Firebox scheme. The width of the firebox is 1000 mm.

The modeling is based on an assumption, that the volatiles created during the pyrolysis of wood, are equally distributed across the grate. Moreover, while the actual grate is equipped with a large number of air nozzles located on its surface, the air inlets were substituted with several inlet gaps of total area equal to the area of all real air nozzles. Combustion of wood volatiles was modeled according to the equation

$$C_xH_yO_z + 1.058O_2 \rightarrow CO_2 + 1.191H_2O\ , \tag{1}$$

with reaction pre-exponential factor of 2.119×10^{11} and activation energy of 2.027×10^8 J/kgmol. Figure 9 presents molar fractions of O_2, CO_2 and H_2O in the outflow plane of the firebox. Normally, the molar fraction of CO_2 in the flue gases should be higher than molar fraction of O_2. In presented case, the amount of air injected exceeds the optimal value as there is more oxygen than carbon dioxide.

Figures 10–17 show the quantitative results of CFD nozzle placement simulations. When only side nozzles are active, the molar fraction of CO_2 is highest

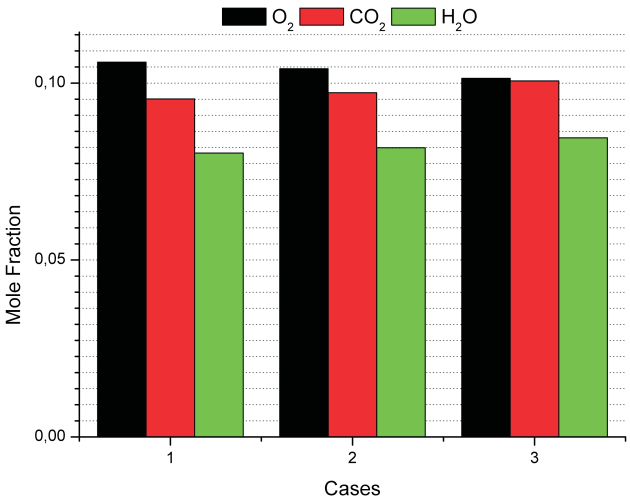

Figure 9. Molar fraction of O_2, CO_2 and H_2O in the outflow plane of the firebox for every case.

in the vicinity of side walls, as well as in the lower front and bottom part of the firebox (case 1 in Figs. 10–11). When only upper nozzles are active, the molar fraction of CO_2 is relatively uniform in the lower part of the firebox (case 3 in Figs. 10–11). The highest molar fraction of O_2 is in the middle part of lower firebox, when only side nozzles are active (case 1 in Figs. 12–13). When only upper nozzles are active, the molar fraction of O_2 is relatively uniform in the middle part of lower firebox.

The character of flow is different in every case. We can see that in cases 1 and 2, where the side nozzles are active, the flow is irregular and more or less random. Case 3, on the other hand, is characterized by more steady and stable flow (Figs. 14–15). Figures 16–19 show the qualitative results of mean velocity's vertical component and temperature along the A and B lines (Fig. 8). In case 1 a reversed flow (negative value of mean velocity's vertical component) is present at the 0.8–1.1 m of height on line B. This means that the reversed flow occurs in the vicinity of the upper part of the horizontal partition (Fig. 16). In case 3 we can observe a reversed flow at the 1.1–1.5 m of height on line B. The reversed flow occurs near the ceiling of the firebox (Fig. 16). We do not observe such phenomena in case 2.

Naturally, the highest temperature is in the lowest part of the firebox, where the fuel reacts with the grate air and with side nozzle's secondary air (if active). In case 1 (only side nozzles are active) the temperature is higher than in case 2 (both side and upper nozzles are active) because less amount of secondary air is delivered through side nozzles than in case 2.

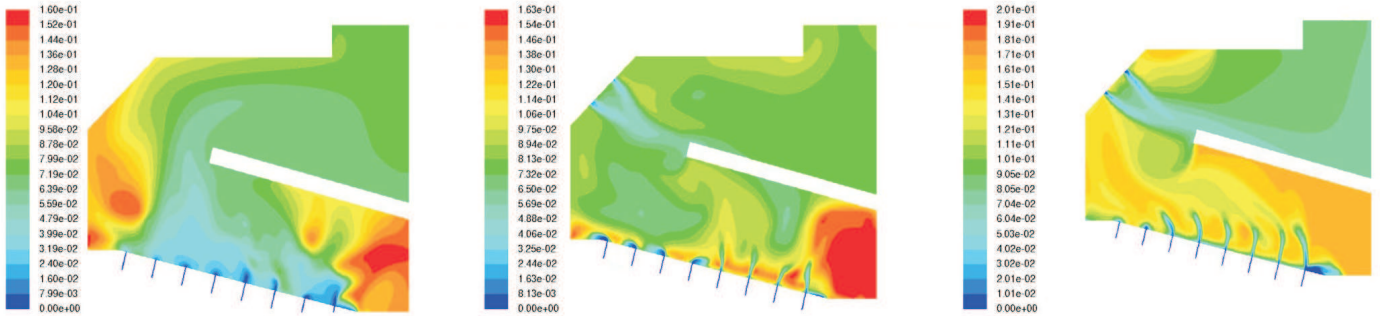

Figure 10. Molar fraction of CO_2 in the symmetry plane of the firebox. From left to right: case 1, case 2, case 3.

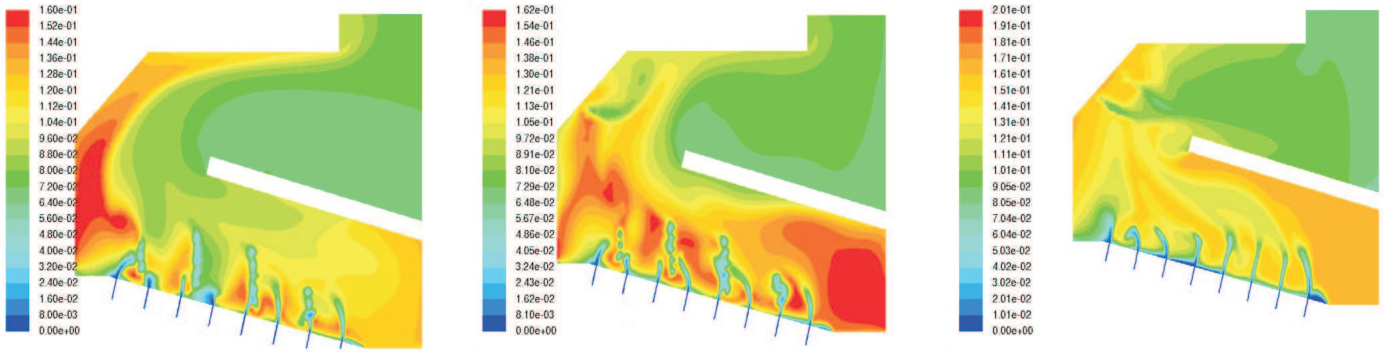

Figure 11. Molar fraction of CO_2 in the plane of 0.10 m offset from the side wall of the firebox. From left to right: case 1, case 2, case 3.

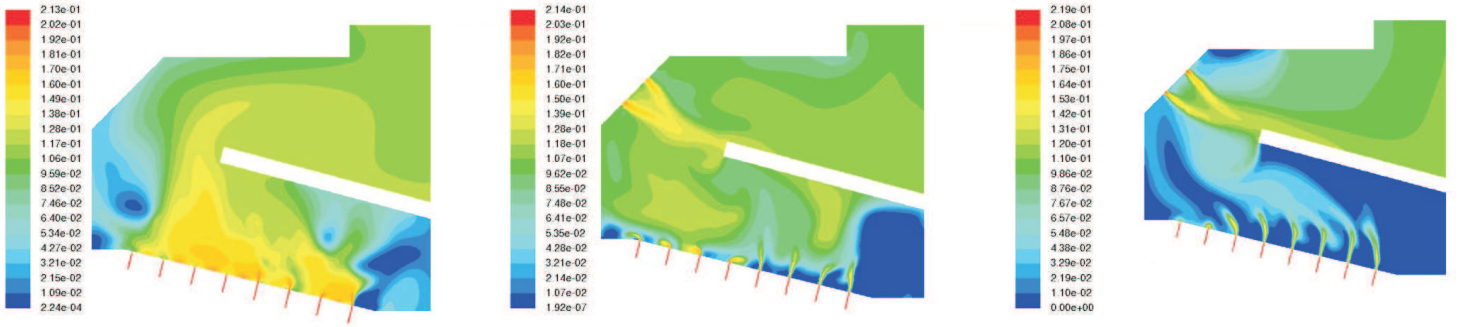

Figure 12. Molar fraction of O_2 in the symmetry plane of the firebox. From left to right: case 1, case 2, case 3.

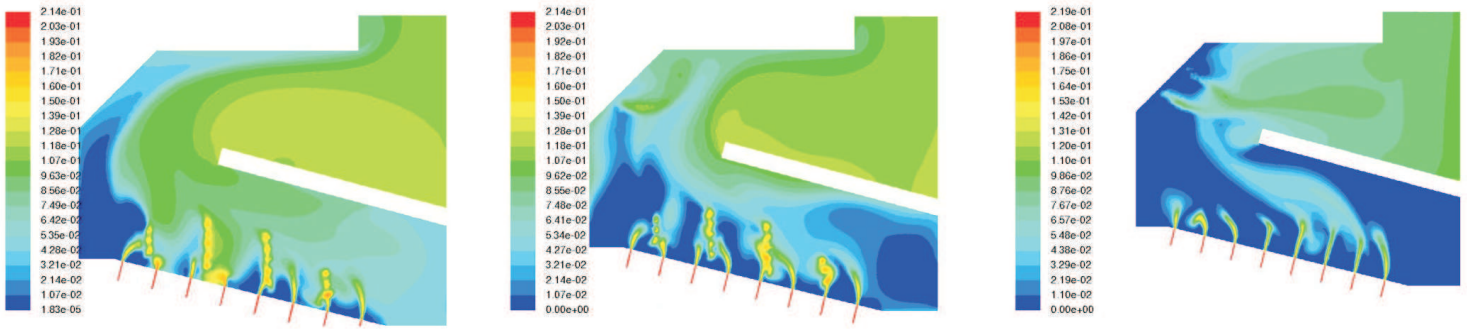

Figure 13. Molar fraction of O_2 in the plane of 0.1 m offset from the side wall of the firebox. From left to right: case 1, case 2, case 3.

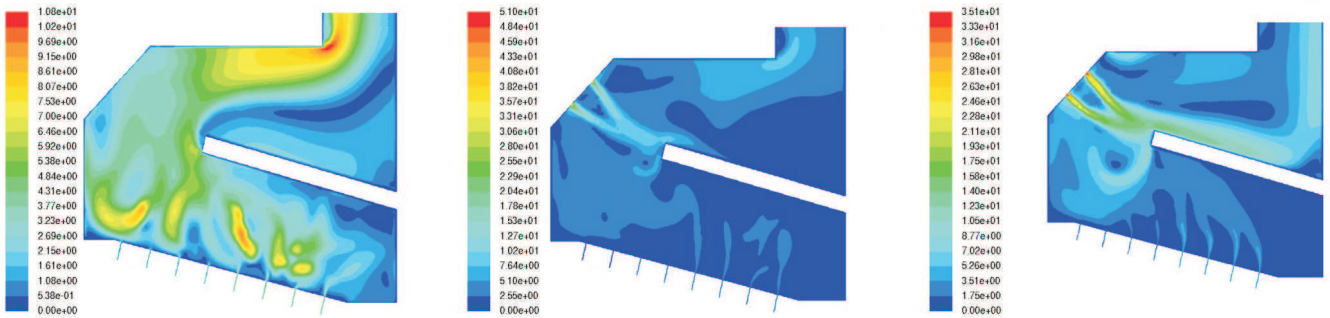

Figure 14. Velocity module in the symmetry plane of the firebox. From left to right: case 1, case 2, case 3.

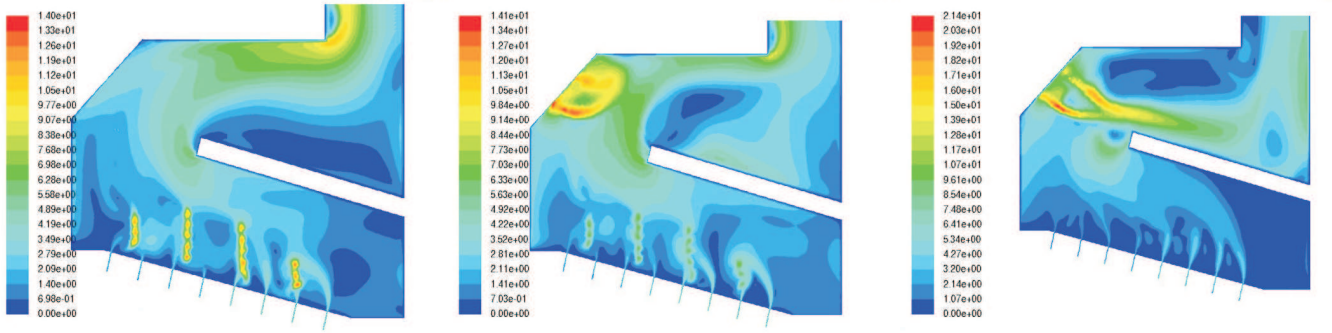

Figure 15. Velocity module in the plane of 0.1 m offset from the side wall of the firebox. From left to right: case 1, case 2, case 3.

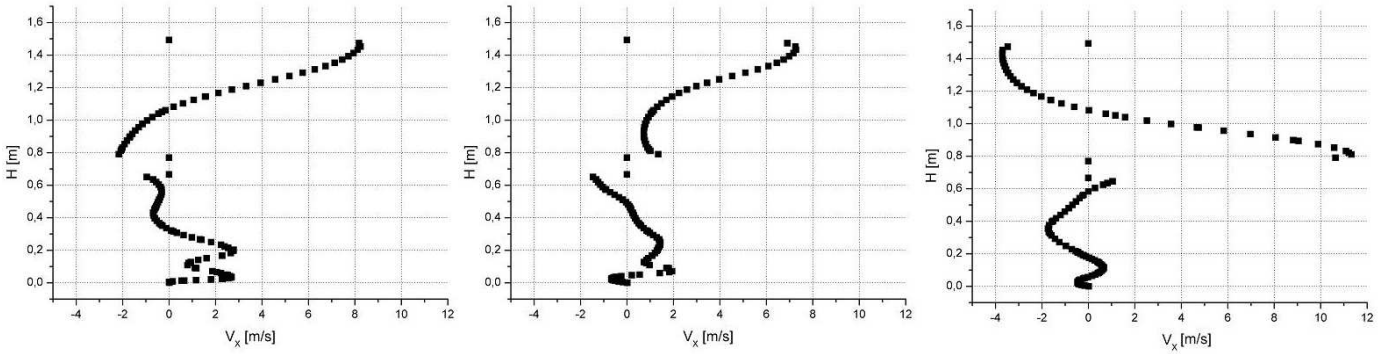

Figure 16. The profile of vertical component of the mean velocity on B line along the height of the firebox (0.35 m from the beginning of the grate, in the symmetry plane, Fig. 8). From left to right: case 1, case 2, case 3.

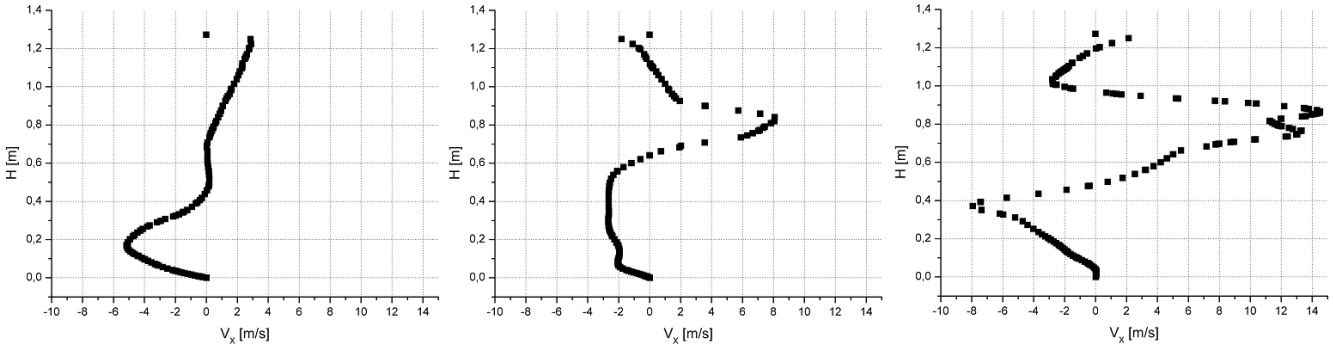

Figure 17. The profile of vertical component of the mean velocity on A line along the height of the firebox (1.25 m from the beginning of the grate, in the symmetry plane, Fig. 8). From left to right: case 1, case 2, case 3.

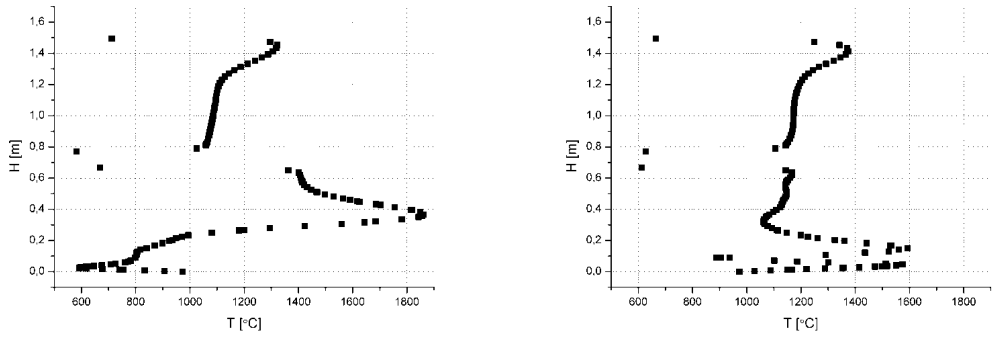

Figure 18. Temperature profile on B line along the height of the firebox (0.35 m from the beginning of the grate, in the symmetry plane, Fig. 8): case 1 (left), case 2 (right).

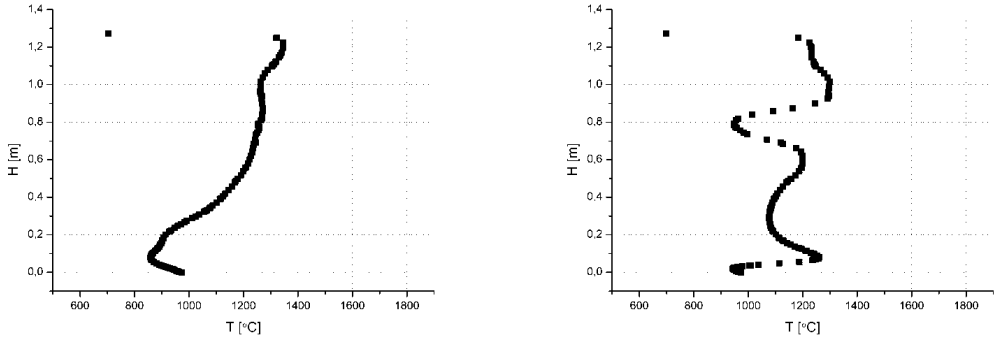

Figure 19. Temperature profile on A line along the height of the firebox (1.25 m from the beginning of the grate, in the symmetry plane, Fig. 8): case 1 (left), case 2 (right).

8 Summary and conclusions

Designed firebox should be able to efficiently burn dry biomass as well as fuel with a high amount of moisture. To deal with it, the combustion chamber was equipped with the moving grate system to ensure optimal drying, gasification and afterburning charcoal. Furthermore, secondary air can be delivered via side as well as upper nozzles independently which provides wide control range and flexibility. The horizontal partition inside the firebox also seems to be a good solution as it ensures a long flue gases' path and their after-burning before reaching the exchanger.

For the investigated firebox geometry, as shown in Figs. 10–15 (case 3), the best solution for efficient burning biomass containing large amounts of moisture

is delivering the secondary air through upper nozzles only. That way we can obtain a long particle residence time inside the firebox. For burning dry biomass, delivering the secondary air via side and upper nozzles simultaneously seems to be the best solution.

The CFD simulations show that the amount of air delivered to the firebox exceeds optimal (Fig. 9). Further calculation with less amount of air should be conducted for higher precision. On the other hand, in order to obtain the best flue gases parameters (such as temperature and molar fraction of CO_2 and H_2O) air should be delivered through both side and upper nozzles.

Acknowledgements The Project is financed by the strategic program of the National Centre for Research and Development (NCBiR) and ENERGA SA: Advanced Technologies for Energy Generation, Task 4: Elaboration of Integrated Technologies for the Production of Fuels and Energy from Biomass, Agricultural Waste and other Waste Materials.

Received 26 March 2013

References

[1] Rokicki H.: *Steam Generators*, Gdańsk University of Technology, Gdańsk 1984 (in Polish).

[2] Kruczek S.: *Boilers. Design and Calculations*. Wrocław University of Technology, Wrocław 2001 in Polish.

[3] Wiśniewski S., Wiśniewski T.S.: *Heat Transfer*. WNT, Warszawa 2000 (in Polish).

[4] Ronewicz K., Turzyński T., Kardaś D., Kulikowicz W., Polesek-Karczewska S., Wardach-Święcicka I., Lampart P.: *Technical documentation of a thermal oil-biomass boiler for 100 kW ORC*. Report IF-FM 49/2013, Gdańsk 2013 (in Polish).

[5] Ronewicz K., Turzyński T., Kardaś D., Wardach-Święcicka I., Kulikowicz W.: *Assumptions for the design of the grate and a system for the boiler supplied with thermal oil*. Rep. IF-FM 623/2012, Gdańsk 2012 (in Polish).

[6] http://www.ansys.com/Products/Simulation+Technology/Fluid+Dynamics/Fluid+Dynamics+Products/ANSYS+Fluent